

# Performance of Adaptive Linear Interference Suppression in the Presence of Dynamic Fading

Michael L. Honig, *Fellow, IEEE*, Scott L. Miller, *Senior Member, IEEE*, Mark J. Shensa, and Lawrence B. Milstein, *Fellow, IEEE*

**Abstract**—Adaptive linear interference suppression for direct-sequence (DS) code-division multiple access (CDMA) is studied in the presence of time- and frequency-selective fading. Interference suppression is achieved with an adaptive digital filter which spans a single symbol interval. Both decision-directed and blind adaptive algorithms, which do not require a training sequence, are considered. Modifications to least squares adaptive algorithms are presented which are compatible with differential coding and detection. For frequency-selective fading, adaptive algorithms are presented based upon different assumptions concerning knowledge of the desired user's channel. Specifically, the cases considered are as follows: 1) perfect knowledge of the desired channel; 2) knowledge of only the relative path delays; and 3) knowledge of only one delay corresponding to the strongest path. Computer simulation results are presented which compare the performance of these algorithms with the analogous RAKE receivers. These results show that for case 3), even slow fading can cause a significant degradation in performance. Effective use of channel parameters in the adaptive algorithm reduces the sensitivity to fade rate, although moderate to fast fading can significantly compromise the associated performance gain relative to the RAKE receiver.

**Index Terms**—CDMA, differential detection, fading, interference suppression, multipath.

## I. INTRODUCTION

LINEAR minimum mean-square-error (MMSE) detection has been proposed as an alternative to the matched filter receiver for direct-sequence (DS) code-division multiple-access (CDMA) systems (see [1, Ch. 6] and [2] and references therein.) A linear MMSE detector can be implemented as an adaptive tapped-delay line, analogous to linear equalizers for single-user channels. Explicit estimates of interference parameters such as relative amplitudes, phases, and spreading codes

are not required for adaptation, given either a training sequence, or knowledge of the desired user's spreading sequence, and associated channel and timing.

If the set of users and channels is time-invariant, then the MMSE solution for the tapped-delay line coefficients corresponding to a particular user can be accurately estimated via conventional adaptive filtering techniques [i.e., stochastic gradient or least squares (LS)]. Unfortunately, this assumption is generally not true for mobile wireless multiple-access systems. Namely, mobility combined with multipath causes dynamic fading, which the adaptive algorithm must track.

Here we examine the performance of adaptive linear interference suppression algorithms for DS-CDMA assuming each user transmits over a Rayleigh fading channel. It has been observed in [3] that conventional adaptive algorithms experience the following problems with frequency-nonselective (flat) Rayleigh fading channels: 1) phase slips which cause the adaptive algorithm to track rotated symbols and 2) false locking onto an interferer, or instability, which can occur during a fade. In [3], phase prediction of the desired symbol is used to solve the first problem. Here we consider two alternative adaptive approaches that do not require phase tracking. The first approach is to use a recursive LS adaptation algorithm with differential decisions as part of the coefficient update. This technique (also considered in [4]) does not preclude the possibility that the algorithm will lock onto an interferer, or become unstable during a fade. The second approach, which does prevent false locking, is to use an orthogonally-anchored algorithm, as described in [5], but modified for differential detection.

Computer simulation results are presented which compare the uncoded performance of adaptive algorithms for the reverse link of a single isolated cell. For the channel model considered, assuming moderate fade rates and uncoded error rates in the range 5%–10%, the numerical results show that the adaptive receivers can accommodate more than twice the number of users as the matched filter in the presence of flat fading.

For frequency-selective fading channels, adaptive algorithms are presented which exploit knowledge of the desired user's channel. The following cases considered are: 1) perfect knowledge of the desired user's channel; 2) knowledge of path delays only (without channel coefficients); and 3) knowledge of only the main (strongest) path delay. Computer simulation results show that MMSE detection (assuming all channels are known) again offers a large increase in the number of users that can be supported. However, multipath fading causes significant performance degradation of the adaptive algorithms, which attempt to estimate the time-varying MMSE solution. At moderate fade

Paper approved by U. Mitra, the Editor for Spread Spectrum/Equalization of the IEEE Communications Society. Manuscript received April 20, 1998; revised February 2, 2000 and September 14, 2000. This work was supported by the National Science Foundation Industry/University Cooperative Research Center on Integrated Circuits and Systems at UCSD, the National Science Foundation under Grant NCR-9628642, the NRad/ONR under Contract 0602232N, and the ARO under Grant DAAH04-96-1-0378. This work was presented in part at the IEEE Vehicular Technology Conference, Phoenix, AZ, 1997, and the International Symposium on Information Theory, Ulm, Germany, 1997.

M. L. Honig is with the Department of Electrical and Computer Engineering, Northwestern University, Evanston, IL 60208 USA (e-mail: mh@ece.nwu.edu).

S. L. Miller is with the Department of Electrical Engineering, Texas A&M University, College Station, TX 77843-3128 USA (e-mail: smiller@ee.tamu.edu).

M. J. Shensa is with SPAWAR, San Diego, CA 92152 USA (e-mail: shensa@nosc.mil).

L. B. Milstein is with the Department of Electrical and Computer Engineering, University of California, San Diego, La Jolla, CA 92093 USA (e-mail: milstein@ece.ucsd.edu).

Publisher Item Identifier S 0090-6778(01)03134-8.

rates, our results show that the adaptive receivers still provide a gain of 1.5–2 in number of users supported relative to the analogous RAKE receivers. In addition, the adaptive receivers are insensitive to near–far power variations over the user population. Our results also show that knowledge of the desired user's channel parameters, such as path delays and path coefficients, can be used to reduce the sensitivity to fade rate.

Before concluding this section, we briefly mention some related work on multiuser detection for fading channels. The combination of noncoherent (differential) and multiuser detection is considered in [6]. The decorrelator [1, ch. 5] is generalized to fading channels in [7] and [8]. Those references do not consider the problem of estimating the detector parameters when the fading is dynamic. In [9] an adaptive blind linear interference suppression filter for multipath channels is derived which does not require knowledge of path coefficients. Here we present a least squares (LS) adaptive algorithm based on this structure, and illustrate the performance of this algorithm in the presence of dynamic fading. Pilot-aided coherent MMSE detection for fading channels, in contrast to the differential detection approach taken here, is studied in [10]. Finally, an analysis of some of the algorithms considered here under different assumptions concerning the fade rate is presented in [11].

The DS-CDMA system model is presented in the next section. Adaptive algorithms and performance results for flat fading are presented in Section III. Algorithms for frequency-selective fading are presented in Section IV, and associated performance results are given in Section V.

## II. SYSTEM MODEL

We consider the reverse link of an isolated cell. The  $k$ th active user transmits a baseband signal

$$x_k(t) = \sum_i A_k d_k(i) p_k(t - iT - \nu_k) \quad (1)$$

where  $d_k(i)$  is the  $i$ th differentially encoded symbol transmitted by user  $k$ ,  $p_k(t)$  is the real-valued spreading waveform associated with user  $k$ , and  $\nu_k$  and  $A_k$  are, respectively, the delay and amplitude associated with user  $k$ . For DS-CDMA

$$p_k(t) = \sum_{i=1}^{N-1} a_k[i] \Psi(t - iT_c) \quad (2)$$

where  $a_k[i] \in \{\pm 1/\sqrt{N}\}$ ,  $i = 0, \dots, N - 1$ , is the real-valued spreading sequence,  $\Psi(t)$  is the chip waveform,  $T_c$  is the chip duration, and  $N = T/T_c$  is the processing gain. Square brackets enclosing the function argument denote chip-rate samples, whereas regular parenthesis are used for symbol-rate samples and continuous time. It is assumed that the same spreading waveform is used for each symbol. (Short spreading codes are a requirement for the adaptive algorithms considered here.)

Let  $\mathbf{r}(i)$  be the  $N$ -vector containing samples at the output of a chip-matched filter during the  $i$ th transmitted symbol, assuming that the receiver is synchronized to the desired user. Letting  $k =$

1 correspond to the user to be detected, for flat fading channels we can write

$$\begin{aligned} \mathbf{r}(i) &= d_1(i) h_1(i) \mathbf{p}_1 \\ &+ \sum_{k=2}^K A_k [h_k(i) d_k(i) \mathbf{p}_k^+ + h_k(i-1) d_k(i-1) \mathbf{p}_k^-] + \mathbf{n}(i) \end{aligned} \quad (3)$$

where  $\mathbf{p}_1$  is the spreading sequence associated with user 1,  $\mathbf{p}_k^+$  and  $\mathbf{p}_k^-$  are  $N$ -vectors associated with the  $k$ th interferer,  $\mathbf{n}(i)$  is the vector of noise samples at time  $i$ , assumed to be white with covariance  $\sigma_n^2 \mathbf{I}$ ,  $h_k(i)$  is the  $i$ th channel coefficient corresponding to user  $k$ , and there are  $K$  users. Because the users are asynchronous, each interferer contributes two interfering vectors. The vectors  $\mathbf{p}_k^+$  and  $\mathbf{p}_k^-$  contain the chip matched-filter output samples within the time window spanned by  $\mathbf{r}(i)$  in response to the inputs  $p_k(t - \nu_k)$  and  $p_k(t + T - \nu_k)$ , respectively [2]. The numerical results in Section IV assume rectangular chip shapes. The receiver is assumed to be synchronized to user 1, so that  $\mathbf{p}_1^+$  is the spreading code for user 1, and  $\mathbf{p}_1^-$  contains only zeros. The sequence of channel coefficients for user  $k$ ,  $\{h_k(i)\}$ , is a complex Gaussian random process obtained by passing complex white Gaussian noise through a filter with (approximate) transfer function  $\alpha/\sqrt{1 - (f/f_d)^2}$  where  $\alpha$  is a normalization constant,  $f_d = v/\lambda$  is the maximum Doppler shift,  $\lambda$  is the wavelength of the carrier frequency, and  $v$  is the speed of the mobile. It is assumed that all channels are constant during each symbol interval.

To model frequency-selective fading, we assume specular multipath components that fade independently. The received signal corresponding to user  $k$  is therefore

$$r_k(t) = \sum_{l=1}^{L_k} h_{k,l}(t) x_k(t - \tau_{k,l}) \quad (4)$$

where  $x_k(t)$  is given by (1), and  $h_{k,l}(t)$  and  $\tau_{k,l}$  are, respectively, the channel coefficient and path delay associated with path  $l$  for user  $k$ , and  $L_k$  is the number of paths for user  $k$ . The receiver is assumed to be synchronized with the main path for user 1, i.e.,  $\tau_{1,1} + \nu_1 = 0$ .

All receivers considered in this paper decide on each transmitted symbol by observing the received signal during a single symbol interval. The vector  $\mathbf{r}(i)$  is again formed by collecting  $N$  samples at the output of the chip-matched filter within the window spanned by  $p_1(t - iT)$ . To write an expression for the received vector  $\mathbf{r}(i)$ , we define the matrices  $\mathbf{P}_k^+$  and  $\mathbf{P}_k^-$  as

$$\mathbf{P}_k^\pm = [\mathbf{p}_{k,1}^\pm, \mathbf{p}_{k,2}^\pm, \dots, \mathbf{p}_{k,L_k}^\pm] \quad (5)$$

where  $\mathbf{p}_{k,l}^+$  and  $\mathbf{p}_{k,l}^-$ ,  $1 \leq k \leq K$ ,  $1 \leq l \leq L$ , are the vectors of chip-matched filter outputs during symbol  $i$  corresponding to the inputs  $p_k(t - iT - \nu_k - \tau_{k,l})$  and  $p_k(t - (i-1)T - \nu_k - \tau_{k,l})$ , respectively, which are associated with path  $l$ . Let

$$\mathbf{s}_k^\pm(i) = \mathbf{P}_k^\pm \mathbf{A}_k \mathbf{h}_k(i) \quad (6)$$

where

$$\mathbf{A}_k = \text{diag}[A_{k,1} \cdots A_{k,L_k}]$$

is the diagonal matrix of amplitudes associated with the paths for user  $k$  (determined by the path delay profile and shadowing for user  $k$ ), and

$$\mathbf{h}_k(i) = [h_{k,1}(i) \cdots h_{k,L_k}(i)]' \quad (7)$$

is the vector of complex path coefficients for user  $k$ , where “ $\prime$ ” denotes transpose. The vector  $\mathbf{s}_1^\dagger(i)$  can be viewed as the time-varying “effective” spreading code for user 1 when the multipath for user 1 is coherently combined. Independent fading on each path implies that  $h_{k,l}(i)$  and  $h_{k,m}(i)$ ,  $l \neq m$ , are independent for all  $i$ .

We will assume that all path delays  $\tau_{k,l} \ll T$ , where  $T$  is the symbol interval. It is then reasonable to ignore intersymbol interference, so that the received vector for the  $i$ th symbol can be written as

$$\mathbf{r}(i) = \sum_{k=1}^K [d_k(i)\mathbf{s}_k^\dagger + d_k(i-1)\mathbf{s}_k^-] + \mathbf{n}(i) \quad (8)$$

which is analogous to the expression for flat fading (3). For the numerical results in Section V we assume that the path delays  $\tau_{k,l} = lT_c$ ,  $l = 1, \dots, L_k$ . (For a general interpretation of this assumption, see [12].) The  $m$ th column of  $\mathbf{P}_k^\pm$ ,  $m > 1$ , is then obtained by shifting the  $(m-1)$ th column down by one sample.

The focus of this work is on the effect of channel fading, so that numerical results presented here assume a fixed user population. Namely, the set of active users does not change during the desired user’s transmission. This assumption is, in general, not true for asynchronous packet CDMA. Related performance results to those presented here which account for interference transients and other-cell interference are presented in [13] and [14].

### III. ADAPTIVE RECEIVERS: FLAT FADING

We begin by examining the performance of some specific adaptive receivers with frequency-nonselctive (flat) Rayleigh fading. This case is simpler than the more interesting case of frequency-selective fading, and gives insight into sources of performance degradation. The approach developed here relies on differential coding and detection with LS adaptive algorithms. Two adaptive algorithms are considered. The first we refer to as differential LS (DLS), since it incorporates the differentially decoded symbol into an LS update. The second is based on the orthogonally-anchored algorithm in [5].

The sequence of received samples is the input to a tapped-delay line with tap spacing  $T_c$ . Denoting the vector of coefficients associated with the tapped-delay line at time  $i$  as  $\mathbf{c}(i)$ , the output of the filter at time  $i$  (corresponding to the  $i$ th transmitted symbol) is

$$y(i) = \mathbf{c}^\dagger(i)\mathbf{r}(i) \quad (9)$$

where  $\mathbf{r}(i)$  is given by (3), and “ $\dagger$ ” denotes Hermitian transpose. The filter  $\mathbf{c}(i)$  spans one symbol interval and has  $N$  components. Throughout the rest of the paper, we will assume that  $\mathbf{c}(i)$  is selected to detect user 1.

Let  $b_1(i)$  be the  $i$ th symbol transmitted by user 1. For MPSK, the differentially encoded signal is  $d_1(i) = b_1(i) d_1(i-1)$ . The

numerical results to be presented assume binary signaling for which the estimate of the source symbol  $b_1(i)$  is then

$$\hat{b}_1(i) = \text{sgn}(\Re[y(i)y^*(i-1)]) \quad (10)$$

where “ $*$ ” denotes complex conjugate.

#### A. MMSE Solution

The adaptive algorithms which follow are based on the MMSE criterion. For coherent detection, the objective is to select  $\mathbf{c}(i)$  to minimize the mean squared error (MSE)  $\epsilon = E[|e(i)|^2]$ , where

$$e(i) = d_1(i) - [\mathbf{c}^\dagger(i)\mathbf{r}(i)]. \quad (11)$$

The solution is

$$\mathbf{c}(i) = \mathbf{R}^{-1}(i)\mathbf{p}_1(i) \quad (12)$$

where

$$\begin{aligned} \mathbf{R}(i) &= E[\mathbf{r}(i)\mathbf{r}^\dagger(i)] \\ &= \sum_{k=1}^K A_k^2 \left( |h_k(i)|^2 \mathbf{P}_k^+ \mathbf{P}_k^{+\dagger} + |h_k(i-1)|^2 \mathbf{P}_k^- \mathbf{P}_k^{-\dagger} \right) \\ &\quad + \sigma_n^2 \mathbf{I} \end{aligned} \quad (13)$$

and

$$\mathbf{p}_1(i) = E[d_1^*(i)\mathbf{r}(i)] = h_1(i)\mathbf{p}_1 \quad (14)$$

assuming  $A_1 = 1$  and  $E[|d_k(i)|^2] = 1$ . With differential detection, we replace the error in (11) by the error

$$e^{(d)}(i) = h_1(i)d_1(i) - [\mathbf{c}^\dagger(i)\mathbf{r}(i)]. \quad (15)$$

That is,  $\mathbf{c}^\dagger(i)\mathbf{r}(i)$  is an estimate of  $h_1(i)d_1(i)$ , and the channel  $h_1(i)$  does not affect the symbol estimate provided that  $h_1(i-1) \approx h_1(i)$ . Minimizing  $E[|e^{(d)}(i)|^2]$  again gives (12), where  $\mathbf{p}_1(i) = |h_1(i)|^2 \mathbf{p}_1$ . Since the scale factor is irrelevant for PSK, we define the MMSE vector with differential detection for flat fading as

$$\mathbf{c}_{\text{MMSE}}(i) = \mathbf{R}^{-1}(i)\mathbf{p}_1. \quad (16)$$

We remark that the error associated with the DLS algorithm which follows is neither the coherent error (11) nor the differential error (15).

#### B. DLS

Before describing the DLS algorithm, we first observe that a conventional recursive LS (RLS) algorithm (i.e., with coherent detection) selects  $\mathbf{c}(i)$  to minimize the LS cost function

$$C = \sum_{m=1}^{i-1} w^{i-m-1} |e(m)|^2 \quad (17)$$

where  $w$  is a constant close to one, chosen to discount past data, and the error  $e(m)$  is given by (11). (The upper limit of the sum is  $i-1$  instead of  $i$ , since  $e(i)$  cannot be computed before  $\mathbf{c}(i)$  is computed.) The  $\mathbf{c}(i)$  which minimizes the LS cost function is

$$\mathbf{c}(i) = \tilde{\mathbf{R}}^{-1}(i)\tilde{\mathbf{p}}_1^{(\text{coh})}(i) \quad (18)$$

where

$$\tilde{\mathbf{R}}(i) = \sum_{m=1}^{i-1} w^{i-m-1} \mathbf{r}(m) \mathbf{r}^\dagger(m) \quad (19)$$

and

$$\tilde{\mathbf{p}}_1^{(\text{coh})}(i) = \sum_{m=1}^{i-1} w^{i-m-1} d_1^*(m) \mathbf{r}(m). \quad (20)$$

Note that  $\tilde{\mathbf{R}}(i)$  and  $\tilde{\mathbf{p}}_1^{(\text{coh})}(i)$  are scaled estimates of  $\mathbf{R}(i-1)$  and  $\mathbf{p}_1(i-1)$  in (13) and (14), respectively. The expression for  $\tilde{\mathbf{p}}_1^{(\text{coh})}$  depends on either a training sequence or estimates of the sequence  $\{d_1(i)\}$ .

The preceding coherent LS algorithm attempts to track the time-varying channel associated with the desired user. Consider the case where there is only one user and no noise, so that  $\mathbf{r}(i) = d_1(i)h_1(i)\mathbf{p}_1$ . If we add a small constant to the diagonal components of  $\hat{\mathbf{R}}$  to ensure invertibility, then it can be shown that the LS estimate reduces to

$$\begin{aligned} \mathbf{c}(i) &= \kappa(i) \tilde{\mathbf{p}}_1^{(\text{coh})}(i) \\ &= \kappa(i) \mathbf{p}_1 \sum_{m=1}^{i-1} w^{i-m-1} \hat{d}_1^*(m) d_1(m) h_1(m) \end{aligned} \quad (21)$$

where  $\hat{d}_1(i)$  is the estimate of  $d_1(i)$  and  $\kappa(i)$  is a real-valued constant which does not affect the error rate. If  $\hat{d}_1(i) = d_1(i)$ , or  $\hat{d}_1(i) = -d_1(i)$  for all  $i$ , then the phase of  $\mathbf{c}(i)$  is a weighted average of the channel fade process. For binary signaling, the occurrence of a cycle slip causes  $\hat{d}_1(i)$  to switch from  $d_1(i)$  to  $-d_1(i)$  or vice versa. In that case, the average in (21) changes sign, so that the phase of  $\mathbf{c}(i)$  experiences a transient shift of  $\pi$ , which introduces additional phase variations in the differential detector.

The preceding discussion indicates that an improvement in performance can be obtained by eliminating the effect of the desired user's channel in the LS update. The DLS algorithm, which follows, replaces  $d_1(m)$  in (20) by  $\hat{y}(i)$ , an estimate of the filter output  $y(i)$  which incorporates the differentially detected symbol  $\hat{b}(i)$ . This substitution helps to reduce the time-variations in the estimated steering vector  $\hat{\mathbf{p}}_1(i)$  due to  $h_1(i)$ .

The DLS algorithm computes  $\mathbf{c}(i)$  recursively as follows:

$$\hat{y}(i) = \hat{b}_1(i) y(i-1) \quad (22)$$

$$\begin{aligned} \hat{\mathbf{p}}_1(i+1) &= (1-w) \hat{y}^*(i) \mathbf{r}(i) + w \hat{\mathbf{p}}_1(i) \\ &\quad (\text{estimate of } E[\hat{y}^*(i) \mathbf{r}(i)]) \end{aligned} \quad (23)$$

$$\begin{aligned} \hat{\mathbf{R}}(i+1) &= (1-w) [\mathbf{r}(i) \mathbf{r}^\dagger(i)] + w \hat{\mathbf{R}}(i) \\ &\quad (\text{estimate of } E[\mathbf{r}(i) \mathbf{r}^\dagger(i)]) \end{aligned} \quad (24)$$

$$\mathbf{c}(i+1) = \hat{\mathbf{R}}^{-1}(i+1) \hat{\mathbf{p}}_1(i+1). \quad (25)$$

The estimate  $\hat{\mathbf{R}}(i)$  in (24) is not equivalent to the expression (19); however, the update (24) was found to cause fewer numerical problems than the analogous update corresponding to (19). The matrix inverse  $\hat{\mathbf{R}}^{-1}(i)$  in (25) can be propagated via the matrix inversion lemma [15, Sec. 13.2], although care must be taken to ensure that the algorithm is numerically stable.

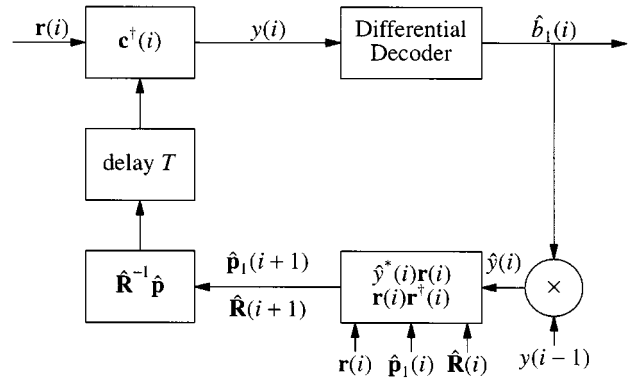


Fig. 1. Block diagram illustrating DLS algorithm.

The DLS algorithm is illustrated in Fig. 1. Consider again the preceding example, where  $\mathbf{r}(i) = d_1(i)h_1(i)\mathbf{p}_1$ . The DLS estimate in this case is

$$\begin{aligned} \mathbf{c}(i) &= \kappa(i) \hat{\mathbf{p}}_1(i) \\ &= \kappa(i) \sum_{m=1}^{i-1} w^{i-m-1} \hat{y}^*(m) \mathbf{r}(m) \\ &= \kappa(i) \sum_{m=1}^{i-1} w^{i-m-1} \hat{b}_1^*(m) [\mathbf{c}^\dagger(m-1) \mathbf{r}(m-1)]^* \mathbf{r}(m) \\ &= \kappa(i) \sum_{m=1}^{i-1} w^{i-m-1} \hat{b}_1^*(m) \\ &\quad \cdot \{d_1(m-1)h_1(m-1) [\mathbf{c}^\dagger(m-1)\mathbf{p}_1]\}^* \\ &\quad \cdot d_1(m)h_1(m)\mathbf{p}_1 \end{aligned} \quad (26)$$

where here we assume the same exponential weighting as in (13) and (14) for the coherent RLS algorithm. If  $h_1(m-1) \approx h_1(m)$  and  $\hat{b}_1(m) = b_1(m)$ , then (26) becomes  $\mathbf{c}(i) = \kappa(i) \mathbf{p}_1 \sum_{m=1}^{i-1} w^{i-m-1} |h_1(m)|^2 [\mathbf{c}^\dagger(m-1)\mathbf{p}_1]$ , in which case the phase of  $\mathbf{c}$  does not depend on the phase of the channel. Specifically,  $\mathbf{c}(m) = \alpha(m)e^{j\theta}\mathbf{p}_1$  is a solution for any fixed phase offset  $\theta$ , where  $\alpha(m)$  is a real-valued scalar. Consequently, with flat fading the DLS algorithm introduces less "phase noise" in the estimate than the conventional coherent RLS algorithm.

### C. Orthogonally-Anchored LS (OALS)

The DLS algorithm solves the phase ambiguity problem associated with fading channels. However, a remaining problem is that since the DLS algorithm is decision-directed (after initial training with a training sequence), a deep fade can cause the algorithm to lose track of the desired user. In principle, the algorithm can lock onto another user who is not experiencing a fade (transient near-far problem). To prevent this from happening, the blind adaptive approach presented in [5] can be used. The vector  $\mathbf{c}(i)$  is written as the sum

$$\mathbf{c}(i) = \mathbf{p}_1 + \mathbf{x}(i) \quad (27)$$

where  $\mathbf{x}(i)$  is constrained to be orthogonal to  $\mathbf{p}_1$ . Selecting  $\mathbf{x}(i)$  to minimize the variance of the output  $E[|\mathbf{c}^\dagger(i)\mathbf{r}(i)|^2]$  is then

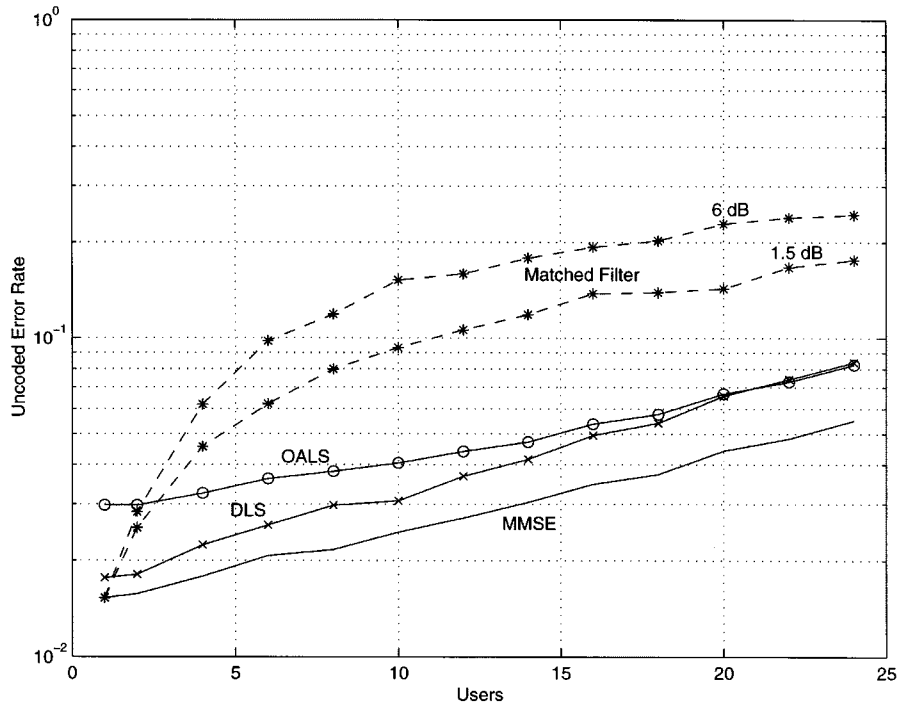


Fig. 2. Unencoded error rate versus users for a single-path Rayleigh fading channel. Results are shown for the following receivers: matched filter (—\*—); DLS (—×—), OALS (—○—); and differential MMSE (—). Two curves are shown for the matched filter corresponding to different standard deviations for log-normal shadowing.  $N = 32$ ,  $E_b/N_0 = 12$  dB,  $f_d T = 0.008$  cycles/symbol for all users.

equivalent to minimizing the interference plus noise at the filter output.

The preceding approach can be used with either coherent or differential detection. With coherent detection (as assumed in [5]),  $\mathbf{p}_1$  in (27) would be replaced by  $h_1(i)\mathbf{p}_1$ . However, this does not change the orthogonality constraint on the filter  $\mathbf{x}(i)$ , since  $\mathbf{p}_1$  and  $h_1(i)\mathbf{p}_1$  define the same subspace. In other words, the space spanned by the desired signal is channel-invariant in the presence of flat fading. The minimum variance solution for  $\mathbf{x}(i)$  (which gives the scaled MMSE solution for  $\mathbf{c}(i)$  [5]) is therefore the same for both coherent and differential detection. A phase-invariant modification of the orthogonally-anchored algorithm in [5] has also been presented for quadrature modulation with complex spreading codes [16].

An LS algorithm based on the preceding approach selects  $\mathbf{x}(i)$  to minimize the cost function

$$C_{oals} = \sum_{m=1}^i w^{i-m} |\mathbf{c}_m^\dagger(i)\mathbf{r}(m)|^2 \quad (28)$$

where  $\mathbf{c}(i)$  is given by (27), and  $\mathbf{c}^\dagger(i)\mathbf{p}_1 = 1$ . [Note that the upper limit of the sum is  $i$  instead of  $i - 1$ , as in (17).] It is easily shown that the solution is

$$\mathbf{c}(i) = \kappa \tilde{\mathbf{R}}^{-1}(i+1)\mathbf{p}_1 \quad (29)$$

where  $\tilde{\mathbf{R}}(i)$  is given by (19) and  $\kappa = 1/(\mathbf{p}_1^\dagger \tilde{\mathbf{R}}^{-1}(i+1)\mathbf{p}_1)$ . The algorithm used to generate the results in the next section replaces  $\tilde{\mathbf{R}}(i)$  by the recursive update (24). The filter output  $\mathbf{c}^\dagger(i)\mathbf{r}(i)$  is an estimate of  $h_1(i)d_1(i)$ , so that differential detection can be used to recover the transmitted symbol sequence.

#### D. Performance Comparison

Fig. 2 shows plots of unencoded error rate versus number of users, assuming that all users experience flat Rayleigh fading. Curves are shown for the matched filter, the adaptive LS algorithms, and the (differential) MMSE detector. (The conventional coherent RLS algorithm (12)–(14) performs poorly at the fade rate simulated, so that the associated results are omitted.) Each point was obtained by averaging over 150 different configurations of users and delays. Spreading codes and delays assigned to each user are randomly selected from uniform distributions. The processing gain  $N = 32$ , and the bit energy-to-noise-density ratio  $E_b/N_0 = 12$  dB, where  $N_0 = 2\sigma_n^2$ .

The average received power for each user is selected from a log-normal distribution. Two curves are shown for the matched filter, corresponding to standard deviations of 1.5 and 6 dB, representing different degrees of closed-loop power control. The remaining curves for the adaptive and MMSE receivers assume a standard deviation of 6 dB.

For the results in Fig. 2, all received signals experience flat Rayleigh fading with a normalized Doppler frequency of  $f_d T = 0.008$  cycles/symbol. In practice, mobile users experience different fade rates, which depend on velocities. These results can therefore be interpreted as worst-case in the sense that all interferers experience the maximum fade rate, which makes it difficult for the adaptive filter to track the optimal solution.

Two parameters for the adaptive algorithms (in addition to the filter length, which is equal to the processing gain) are the training period and the exponential weighting factor  $w$ . We set  $w = 0.998$  (corresponding to an averaging window length of approximately  $1/(1-w) = 500$  symbols), which appeared to be about optimal. The initial training time was 400 symbols. The

initial values of  $\hat{\mathbf{R}}$  and  $\hat{\mathbf{p}}$  were taken to be  $0.01 \times \mathbf{I}$  and the vector of zeros, respectively. Performance was relatively insensitive to this choice.

We observed that the fading process occasionally caused the DLS algorithm to become unstable. To prevent this from happening, the error rate was monitored over a sliding window of 400 symbols. Whenever the error rate exceeded 15%, the DLS algorithm was replaced by the orthogonally-anchored blind algorithm. This switch occurred relatively infrequently, but significantly affected performance when the number of users/cell was moderate to large (i.e.,  $>6$ ). It has been observed in [4] that normalizing the filter (e.g., to unit length) helps to improve the robustness of the DLS algorithm, and may eliminate the need to switch to the blind algorithm.

Fig. 2 shows that the adaptive receivers with loose power control offer a significant increase in capacity at moderate error rates (between a factor of 2 and 3) when compared with the matched filter with tight power control. Further simulations show that the performance of the adaptive algorithms is relatively insensitive to the standard deviation of received powers.

Fig. 2 also shows that the error rate for the DLS algorithm is close to the MMSE lower bound. This may seem surprising given that the fade rate is relatively fast, making it difficult for the adaptive algorithms to track the user channels. To see why the algorithms perform close to the MMSE solution, consider the zero-forcing, or decorrelating, solution for the filter vector  $\mathbf{c}(i)$ . This solution is the orthogonal projection of the desired user's spreading code onto the space spanned by the interferers. Since this solution depends only on the subspaces spanned by the desired user and the interferers, it does not depend on the channel coefficients, and is therefore time-invariant. Consequently, when the number of users per cell is relatively small, the filter has a sufficient number of degrees of freedom to suppress all users, and does not need to track the channels. As the number of users increases, however, the filter can only suppress a subset of strongest interferers, which is time-varying. This leads to the degradation in performance relative to the MMSE solution, which is shown in Fig. 2.

The preceding explanation does not apply to multipath channels, since in that case the subspace spanned by each user does depend on the channel coefficients associated with each path. In other words, the zero-forcing solution is time-varying, which creates a significant tracking problem.

#### IV. ADAPTIVE RECEIVERS: FREQUENCY-SELECTIVE FADING

In this section, we present adaptive algorithms for multipath channels. Three different cases are considered, corresponding to different *a priori* knowledge of the desired user's channel. The cases are as follows: 1) known path delays and channel coefficients; 2) known path delays with unknown channel coefficients; and 3) timing for only the strongest path with unknown channel coefficients. The first case is relevant when the receiver is able to estimate the channel of the desired user from a pilot signal. The second case is relevant when the receiver is able to track path delays but not the channel coefficients. Finally, in the third case the channel estimation is performed implicitly by the adaptive algorithm. In each case, we also specify the corre-

sponding RAKE receiver [17, Sec. 14-5-2] with which the adaptive receiver is compared.

##### A. Known Channel

If the channel for the desired user is known, then the (single-path) matched filter can be replaced by a maximal-ratio RAKE combiner [17, Sec. 14-5-2]. Since the filter observation window spans one symbol, the max-ratio RAKE combiner is specified by the filter

$$\mathbf{c}(i) = \mathbf{P}_1 \mathbf{h}_1(i) \quad (30)$$

where  $\mathbf{P}_1 = \mathbf{P}_1^+$  and  $\mathbf{h}_1$  are defined by (5) and (7), respectively. For the numerical results in Section V, the path delays are fixed for the duration of the desired user's transmission.

For this case, the time-varying MMSE solution for the filter coefficients is

$$\mathbf{c}(i) = \mathbf{R}^{-1}[\mathbf{P}_1 \mathbf{h}_1(i)] \quad (31)$$

where

$$\begin{aligned} \mathbf{R}(i) &= E[\mathbf{r}(i)\mathbf{r}^\dagger(i)] \\ &= \sum_{k=1}^K [\mathbf{P}_k^+ |\mathbf{H}_k(i)|^2 (\mathbf{P}_k^+)^{\dagger} + \mathbf{P}_k^- |\mathbf{H}_k(i)|^2 (\mathbf{P}_k^-)^{\dagger}] + \sigma_n^2 \mathbf{I} \end{aligned} \quad (32)$$

and

$$\mathbf{H}_k(i) = \text{diag}[h_{k,1}(i), \dots, h_{k,L_k}(i)]. \quad (33)$$

The corresponding coherent LS adaptive filter is then

$$\mathbf{c}(i) = \hat{\mathbf{R}}^{-1}(i) [\mathbf{P}_1 \mathbf{h}_1(i)] \quad (34)$$

where the estimate  $\hat{\mathbf{R}}$  is given by (24). This has the interpretation of minimizing filter output variance subject to the orthogonal decomposition (27), where  $\mathbf{p}_1$  is replaced by  $\mathbf{P}_1 \mathbf{h}_1(i)$ . In other words, this is equivalent to the LS orthogonally anchored blind algorithm described in Section III, where the anchor is now the time-varying max-ratio RAKE combiner.

Here we do not consider the effect of inaccurate channel measurements on the performance of the preceding algorithm. This has the same effect as that of a mismatched anchor, which was studied in [5]. A blind technique for estimating the desired user's channel which can significantly reduce the degradation due to mismatch has been presented in [18].

We remark that other adaptive receivers have been proposed for the case considered. Namely, in [19] and [20], separate symbol-length adaptive filters are used for each multipath component. This is more complex than the single filter represented by (34). Furthermore, a problem with this approach is that multipath from the desired user acts as additional correlated interference, which can degrade the performance of the adaptive algorithm at moderate fade rates (see the discussion in the next section.)

##### B. Known Path Delays, Unknown Coefficients

We now assume that the path delays  $\tau_{1,l}$  are known, but that the channel coefficients  $h_{1,l}$  are unknown for  $l = 1, \dots, L_1$ .

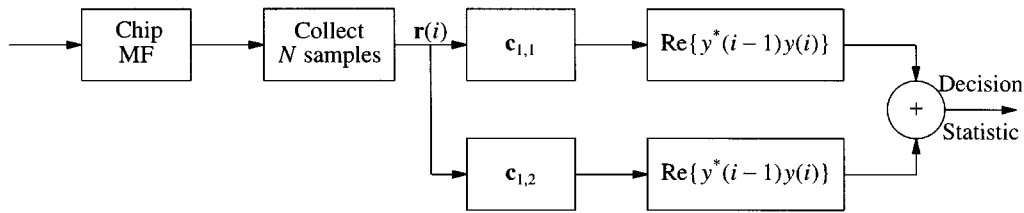


Fig. 3. EG RAKE (noncoherent combiner).

In this case, the (single-path) matched filter can be replaced by a noncoherent equal-gain (EG) RAKE combiner [17, Sec. 15-4-2]. Fig. 3 shows this structure for two paths, where for the conventional RAKE combiner,  $\mathbf{c}_{1,m} = \mathbf{p}_{1,m}$ ,  $m = 1, 2$ .

In addition to the noncoherent RAKE combiner, we will also consider an *adaptive* LS RAKE combiner, which estimates the channel coefficients  $\mathbf{h}_1$  for coherent combining. Specifically, the LS RAKE combiner is defined by the filter

$$\mathbf{c}(i) = \mathbf{P}_1 \hat{\mathbf{h}}_1(i) \quad (35)$$

where  $\hat{\mathbf{h}}_1(i)$  is selected to minimize the LS cost function (17). The solution is

$$\hat{\mathbf{h}}_1(i) = \left( \mathbf{P}_1^\dagger \hat{\mathbf{R}}(i) \mathbf{P}_1 \right)^{-1} \mathbf{P}_1^\dagger \hat{\mathbf{p}}_1(i) \quad (36)$$

where

$$\hat{\mathbf{p}}_1(i) = (1-w)\hat{\mathbf{p}}_1(i-1) + w\hat{d}_1^*(i)\mathbf{r}(i). \quad (37)$$

The MMSE solution for  $\hat{\mathbf{h}}_1(i)$  is not the same as the max-ratio combiner  $\mathbf{h}_1(i)$  when interference is present. That is, the adaptive RAKE is capable of limited interference suppression. For the numerical results in the next section, we assume correct decisions, i.e.,  $\hat{d}_1(i) = d_1(i)$  in (37), such as if a pilot were present. This enables performance close to the max-ratio combiner for the fade rates considered.

To suppress multiple-access interference, each matched filter in Fig. 3 can be replaced by an adaptive filter using the DLS algorithm. However, multipath from the desired user acts as correlated interference which adversely affects convergence and tracking. Specifically, for the case considered with low delay spread, this technique performs no better than the DLS algorithm, since each adaptive filter approximates the same DLS filter.

To avoid the preceding problem, each adaptive filter must isolate a single multipath component. That is, the adaptive algorithm must not “see” the other paths from the desired user. Such a noncoherent EG combiner has been presented in [9]. Namely, referring to Fig. 3, we write  $\mathbf{c}_{1,l} = \mathbf{p}_{1,l} + \mathbf{x}_l$ , where  $\mathbf{x}_l$  is selected to minimize output variance. To isolate the  $l$ th path, the adaptive filter must be constrained to be orthogonal to the *space* spanned by the desired signal. That is

$$\mathbf{x}_l^\dagger \mathbf{P}_1 = \mathbf{0}, \quad l = 1, \dots, L_1. \quad (38)$$

Let

$$\mathbf{C} = [\mathbf{c}_{1,1} \dots \mathbf{c}_{1,L_1}] \quad (39)$$

( $N \times L_1$  matrix). Then (38) is equivalent to the constraint

$$\mathbf{C}^\dagger \mathbf{P}_1 = \mathbf{P}_1^\dagger \mathbf{P}_1. \quad (40)$$

To derive an adaptive algorithm we select  $\mathbf{C}$  to minimize the cost function

$$\mathcal{C} = \sum_{m=1}^i w^{i-m} \|\mathbf{C}^\dagger(i)\mathbf{r}(i)\|^2 \quad (41)$$

subject to the constraint (40). The solution is

$$\mathbf{C}(i) = \hat{\mathbf{R}}^{-1}(i) \mathbf{P}_1 \left( \mathbf{P}_1^\dagger \hat{\mathbf{R}}^{-1}(i) \mathbf{P}_1 \right)^{-1} \left( \mathbf{P}_1^\dagger \mathbf{P}_1 \right). \quad (42)$$

Each filter  $\mathbf{c}_{1,l}$  minimizes interference plus noise from *other* users at the filter output. We will refer to this receiver as the equal-gain LS (EGLS) receiver. Unlike the orthogonally-anchored algorithm for flat fading, the corresponding minimum variance solution (where  $\mathbf{R}$  replaces  $\hat{\mathbf{R}}$ ) does not minimize MSE.

In practice, timing offset, or imprecise knowledge of path delays and delay spread, can compromise the performance of the preceding algorithms. Namely, these inaccuracies create mismatch between the transmitted pulse and the matched filter anchors  $\{\mathbf{p}_{1,1}, \dots, \mathbf{p}_{1,L_1}\}$ . We do not study the effect of this mismatch here, although we remark that the effect of this mismatch can be minimized by estimating the path delays to maximize the cost function (41). (Once the first path delay is selected, the remaining path delays can be constrained to be integer multiples of  $T_c$  [12].) The effect of timing offset on the performance of LS adaptive algorithms in the absence of fading is considered in [14].

### C. Known Delay for Main Path

In this case, the matched filter is a single correlator for the main path. In practice, some form of RAKE combining is generally used with multipath, so we omit numerical performance results for the single-path correlator. The corresponding adaptive receiver is the DLS algorithm presented in Section III. For very slow fading, the DLS algorithm can track the desired user’s channel, and in principle, achieves the same performance as the MMSE filter (31) with differential detection.

## V. PERFORMANCE COMPARISON: FREQUENCY-SELECTIVE FADING

Figs. 4–6 show performance results (uncoded error rate) for the receivers discussed in Section IV and described in Table I. (Not all receivers are represented in Figs. 4 and Fig. 6.) In the table, the receivers are grouped according to the following categories: RAKE, adaptive, and optimal (known channel parameters for all users). In the figures, solid lines correspond to noncoherent receivers and dashed lines correspond to coherent receivers.

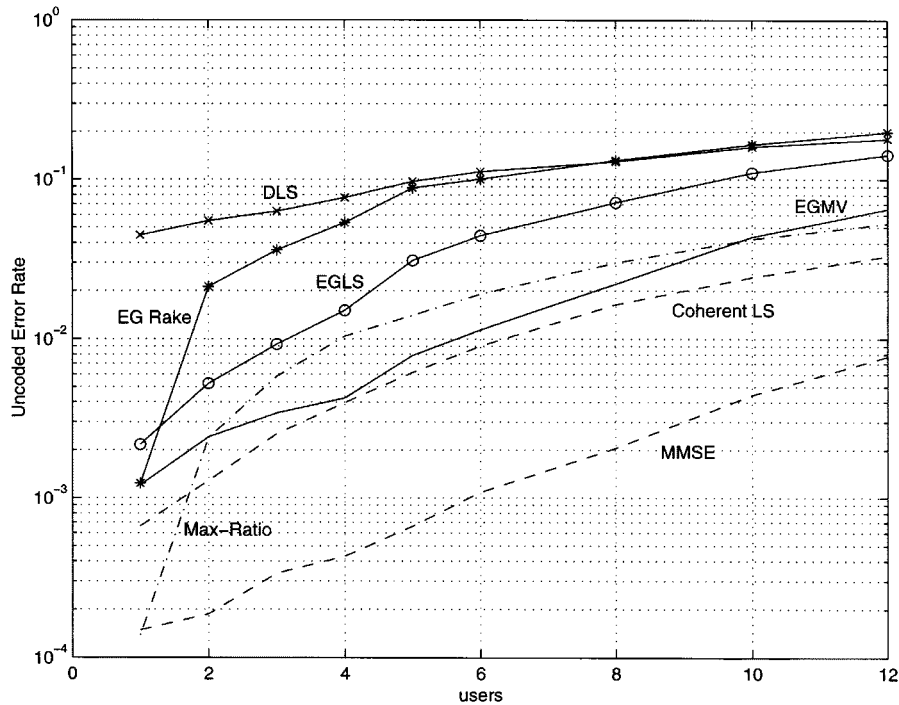


Fig. 4. Uncoded error rate versus number of users for a three-path Rayleigh fading channel. Results are shown for the following receivers: Equal Gain (EG) RAKE ( $- * -$ ), DLS ( $- \times -$ ), EGLS ( $- o -$ ), Equal Gain Minimum Variance (EGMV) ( $-$ ), Maximal-Ratio RAKE ( $-$ ), coherent LS with known channel ( $- \times -$ ), and MMSE ( $- -$ ).  $N = 16$ ,  $E_b/N_0 = 12$  dB,  $f_d T = 0.004$  cycles/symbol.

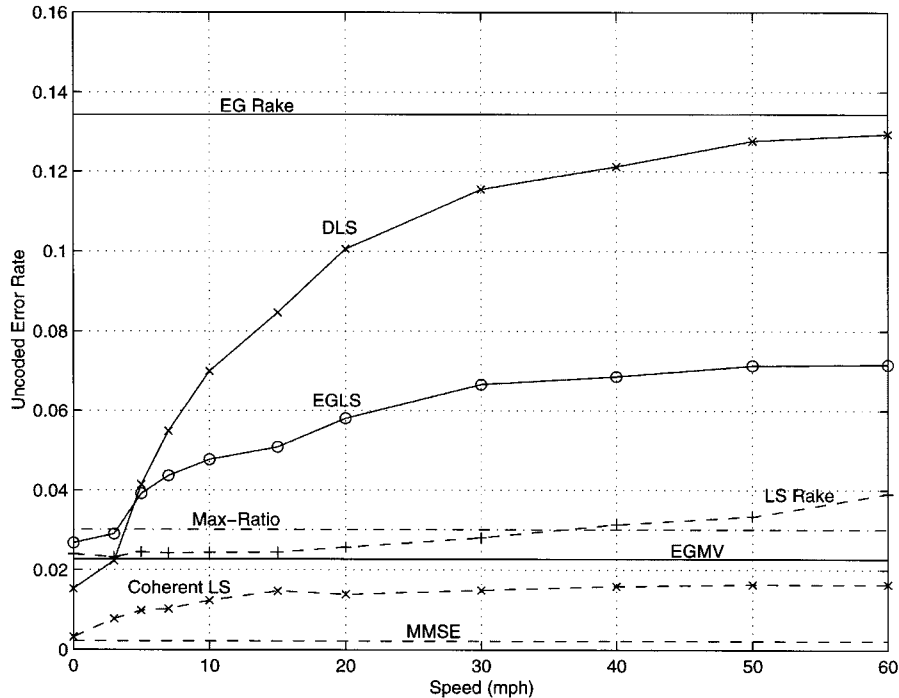


Fig. 5. Uncoded error rate versus mobile speed (mi/h) for a three-path Rayleigh fading channel. Results are shown for the following receivers: Equal Gain RAKE ( $-$ ), LS Adaptive RAKE ( $- - + - -$ ), DLS ( $- \times -$ ), EGLS ( $- o -$ ), EGMV ( $-$ ), Maximal-Ratio ( $-$ ), coherent LS with known channel ( $- \times -$ ), and MMSE ( $- -$ ).  $N = 16$ ,  $K = 8$  users,  $E_b/N_0 = 12$  dB.

In each figure, the processing gain  $N = 16$ , and the channel for each user consists of three independent Rayleigh fading paths of equal power separated by  $T_c$ . For all receivers, the standard deviation of received powers is 1.5 dB for each path. Specifically, the average power of the primary path for each user is selected from a log-normal distribution, and

the remaining paths have the same averaged power. Further simulations with an exponentially decaying power delay profile indicate that with many interferers, the relative performance of the algorithms is insensitive to the attenuation on successive paths. Each simulated point in the plots that follow represent an average over randomly assigned spreading codes and

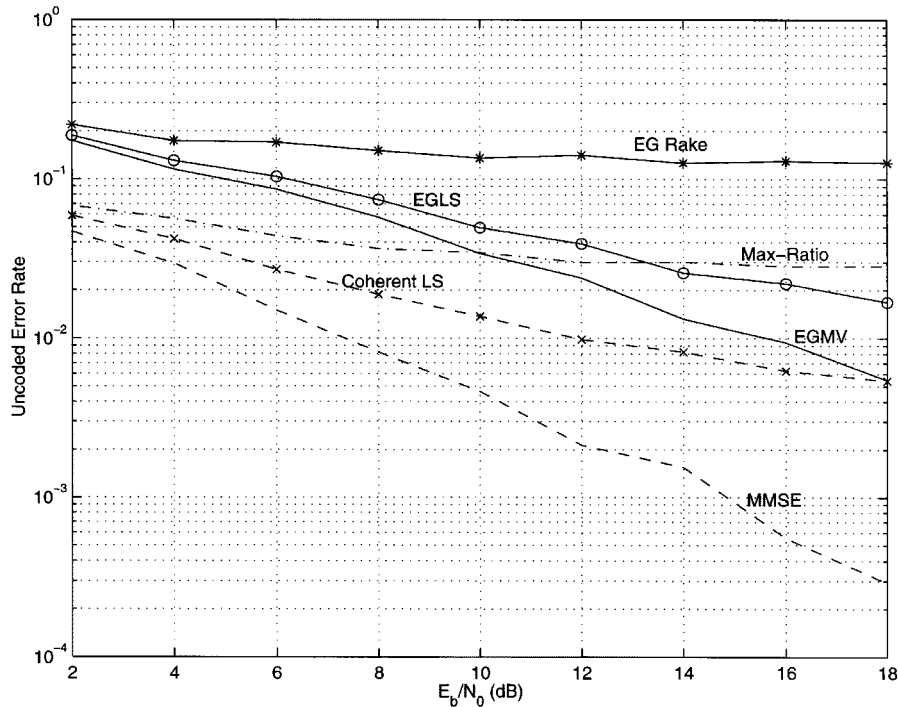


Fig. 6. Uncoded error rate versus  $E_b/N_0$  for a three-path Rayleigh fading channel. Results are shown for the following receivers: Equal Gain RAKE ( $- * -$ ), EGLS ( $- o -$ ), EGMV ( $- \times -$ ), Maximal-Ratio ( $- \cdot -$ ), coherent LS with known channel ( $- \times -$ ), and MMSE ( $- \cdot -$ ).  $N = 16$ ,  $K = 8$  users,  $1/(f_d T) = 1500$  symbols/fade cycle.

TABLE I

ALGORITHMS USED TO GENERATE THE SIMULATION RESULTS IN SECTION V. THE ENTRIES "PATH DELAYS" AND "COEFFICIENTS" REFER TO THE CHANNEL FOR THE DESIRED USER, WHEREAS "ALL CHANNELS" MEANS THAT CHANNELS FOR ALL USERS MUST BE KNOWN TO COMPUTE THE CORRESPONDING RECEIVER FILTER

Algorithm	Category	Filter Coefficients $c(i)$	Coherent/Noncoherent	Side Information
Maximal-Ratio	Rake	$\mathbf{P}_1 \mathbf{h}_1(i)$ (30)	coherent	path delays, coefficients
Equal-Gain (EG) Rake	Rake	See Figure 3: $\mathbf{c}_{1,m} = \mathbf{p}_{1,m}$	noncoherent	path delays
LS Rake	Rake	$\mathbf{P}_1 \mathbf{h}_1(i)$ (35)-(37)	coherent	path delays
Coherent LS (known channel)	Adaptive	$\mathbf{R}^{-1}[\mathbf{P}_1 \mathbf{h}_1(i)]$ (34)	coherent	path delays, coefficients
Equal-Gain LS (EGLS)	Adaptive	See (42) and Figure 3	noncoherent	path delays
Differential Least Squares (DLS)	Adaptive	$\mathbf{R}^{-1}(i) \hat{\mathbf{p}}_1(i)$ (22)-(25)	noncoherent	main path delay
MMSE	Optimal	$\mathbf{R}^{-1}[\mathbf{P}_1 \mathbf{h}_1(i)]$ (31)	coherent	all channels ( $\mathbf{R}$ )
Equal Gain Minimum Variance (EGMV)	Optimal	(42) where $\mathbf{R}$ replaces $\hat{\mathbf{R}}$	noncoherent	all channels ( $\mathbf{R}$ )

delays. For the DLS algorithm, the receiver is assumed to be synchronized to the first path.

Fig. 4 shows uncoded error rate versus number of users. In this figure, the normalized Doppler shift is  $f_d T = 0.004$  (half of that corresponding to Fig. 2). Even at this moderate fade rate, the DLS algorithm performs much worse than the MMSE receiver with differential detection, which indicates that it is unable to track the user channels. The noncoherent EGLS algorithm gives an increase in number of users between 1.5–2 relative to the EG RAKE at moderate error rates. This gain in capacity increases as the fade rate decreases, and as the standard deviation of received

powers increases. The EG minimum variance (EGMV) curve corresponds to perfect knowledge of the interferer channels. The gap between the EGLS and EGMV curves is therefore due to tracking error. We also observe from Fig. 4 that the coherent LS algorithm gives a modest (but significant) gain in number of users that can be supported relative to the max-ratio RAKE combiner. The performance of the LS RAKE receiver is similar to that of the maximal-ratio combiner and is not shown in this figure.

As the fade rate tends to zero, the error rates for the coherent LS and EGLS algorithms approach those for the MMSE and

EGMV receivers, respectively. The error rate for the DLS algorithm approaches that of the MMSE receiver with differential detection. This is illustrated in Fig. 5, which shows uncoded error rate versus mobile speed, assuming a carrier frequency  $f_c = 900$  MHz and data rate of 19.2 kb/s. (The results in Fig. 4 correspond to a mobile speed of 30 mi/h.) This figure indicates that in order for the DLS algorithm to track the MMSE solution with significant accuracy, the fade rate must be very slow. (Even 5 mi/h causes substantial degradation.) In contrast, the adaptive RAKE is able to track the channel for the fade rates considered since only three coefficients are being estimated (instead of 16 for the DLS algorithm), and a smaller exponential weight can be used ( $w = 0.95$  for the results shown). With slow fading, Fig. 5 shows that the LS RAKE performs somewhat better than the max-ratio combiner. The noncoherent EGLS algorithm is less sensitive to the fade rate than is the DLS algorithm, although there is still significant degradation relative to the minimum variance solution at moderate to fast fade rates.

Fig. 6 shows plots of error rate versus SNR for the receivers considered. The corresponding curve for the DLS algorithm is nearly the same as the EGLS curve, and is therefore omitted. The fade rate for this set of curves is  $1/(f_d T) = 1500$  symbols/fade cycle, which corresponds to a mobile speed of 5 mi/h in Fig. 5. These results show that there is an error floor for the RAKE receivers due to interference, in contrast to the adaptive and optimal receivers, which are not interference-limited. We also note that for the three-path channel simulated, there is a large gap between the noncoherent EGMV and coherent MMSE curves (8 dB at an error rate of  $10^{-2}$ ).

## VI. CONCLUSIONS

Adaptive interference suppression algorithms for dynamic fading channels based on LS cost functions have been presented. Both noncoherent differential detection and coherent detection with known channel parameters have been considered. For flat fading channels, numerical results show that these algorithms can support two to three times more users than the conventional matched filter. Furthermore, performance is an insensitive function of fade rate. When multipath fading is present, the performance of the adaptive receivers depends on the fade rate of the interferers as well as the fade rate of the desired user. Numerical results indicate that significant performance degradation occurs relative to the optimal time-varying solution unless the fading is very slow (more than 2000 symbols per average fade cycle). Knowledge of the desired user's channel reduces this sensitivity, and when combined with the adaptive interference suppression algorithms presented here, can provide significant gains relative to the analogous RAKE receivers. Moreover, adaptive receivers are insensitive to received near-far power variations over the user population.

## REFERENCES

- [1] S. Verdú, *Multuser Detection*. Cambridge, U.K.: Cambridge Univ. Press, 1998.
- [2] M. L. Honig and H. V. Poor, "Adaptive interference mitigation in wireless communications systems," in *Wireless Communications: A Signal Processing Perspective*, H. V. Poor and G. Wornell, Eds. Englewood Cliffs, NJ: Prentice-Hall, 1998.

- [3] A. N. Barbosa and S. L. Miller, "Adaptive detection of DS-CDMA signals in fading channels," *IEEE Trans. Commun.*, vol. 46, pp. 115–124, Jan. 1998.
- [4] L. J. Zhu and U. Madhow, "Adaptive interference suppression for direct sequence CDMA over severely time-varying channels," in *Proc. 1997 GLOBECOM*, Phoenix, AZ, Dec. 1997, pp. 917–922.
- [5] M. L. Honig, U. Madhow, and S. Verdú, "Blind adaptive multiuser detection," *IEEE Trans. Inform. Theory*, vol. 41, pp. 944–960, July 1995.
- [6] M. K. Varanasi, "Noncoherent detection in asynchronous multiuser channels," *IEEE Trans. Inform. Theory*, vol. 39, pp. 157–176, Jan. 1993.
- [7] Z. Zvonar and D. Brady, "Multiuser detection in single-path Rayleigh fading channels," *IEEE Trans. Commun.*, vol. 42, pp. 1729–1739, Apr. 1994.
- [8] ———, "Suboptimum multiuser detector for frequency-selective Rayleigh fading synchronous CDMA channels," *IEEE Trans. Commun.*, vol. 43, pp. 154–157, Feb./Mar./Apr. 1995.
- [9] H. C. Huang and S. Verdú, "Linear differentially coherent multiuser detection for multipath channels," *Wireless Pers. Commun.*, vol. 6, no. 1–2, pp. 113–116, Jan. 1998.
- [10] X. Wang and H. V. Poor, "Adaptive joint multiuser detection and channel estimation for multipath fading CDMA channels," *ACM/Baltzer Wireless Networks*, vol. 4, pp. 453–470, 1998.
- [11] S. L. Miller, M. L. Honig, and L. B. Milstein, "Performance analysis of MMSE receivers for DS-CDMA in frequency-selective fading channels," *IEEE Trans. Commun.*, vol. 48, pp. 1919–1929, Nov. 2000.
- [12] M. K. Tsatsanis and G. B. Giannakis, "Optimal linear receivers for DS-CDMA systems: A signal processing approach," *IEEE Trans. Signal Processing*, pp. 3044–3055, 1996.
- [13] M. L. Honig, M. J. Shensa, S. L. Miller, and L. B. Milstein, "Performance of adaptive linear interference suppression for DS-CDMA in the presence of flat rayleigh fading," in *Proc. IEEE Vehicular Technology Conf.*, Phoenix, AZ, May 1997, pp. 2191–2195.
- [14] M. L. Honig, "Adaptive linear interference suppression for packet DS-CDMA," *Eur. Trans. Telecommun.*, vol. 9, no. 2, Mar.–Apr. 1998.
- [15] S. Haykin, *Adaptive Filter Theory*. Englewood Cliffs, NJ: Prentice-Hall, 1994.
- [16] R. de Gaudenzi, F. Giannetti, and M. Luise, "Design of a low-complexity adaptive interference-mitigating detector for DS/SS receivers in CDMA radio networks," *IEEE Trans. Commun.*, vol. 46, pp. 125–134, Jan. 1998.
- [17] J. G. Proakis, *Digital Communications*. New York: McGraw-Hill, 1995.
- [18] M. K. Tsatsanis and Z. Xu, "Performance analysis of minimum variance CDMA receivers," *IEEE Trans. Signal Processing*, vol. 46, pp. 3014–3022, Nov. 1998.
- [19] M. Juntti and M. Latva-aho, "Modified adaptive LMMSE receiver for DS-CDMA systems in fading channels," in *Proc. 1997 PIMRC*, Helsinki, Finland, Sept. 1997.
- [20] M. Latva-aho, "Advanced receivers for wideband CDMA systems," Ph.D. dissertation, Univ. Oulu, Oulu, Finland, 1998.



**Michael L. Honig** (S'80–M'81–SM'92–F'97) received the B.S. degree in electrical engineering from Stanford University, Stanford, CA, in 1977, and the M.S. and Ph.D. degrees in electrical engineering from the University of California, Berkeley, in 1978 and 1981, respectively.

He subsequently joined Bell Laboratories, Holmdel, NJ, where he worked on local area networks and voiceband data transmission. In 1983, he joined the Systems Principles Research Division at Bellcore, where he worked on digital subscriber lines and wireless communications. He was a Visiting Lecturer at Princeton University, Princeton, NJ, during the fall of 1993. Since the Fall of 1994, he has been with Northwestern University, Evanston, IL, where he is a Professor in the Electrical and Computer Engineering Department.

Dr. Honig was an Editor for the IEEE TRANSACTIONS ON INFORMATION THEORY and the IEEE TRANSACTIONS ON COMMUNICATIONS, and a Guest Editor for the *European Transaction on Telecommunications and Wireless Personal Communications*. He was also a member of the Digital Signal Processing Technical Committee for the IEEE Signal Processing Society. He is currently serving as a member of the Board of Governors for the Information Theory Society.



**Scott L. Miller** (S'87–M'88–SM'97) was born in Los Angeles, CA, in 1963. He received the B.S., M.S., and Ph.D. degrees in electrical engineering from the University of California at San Diego (UCSD), La Jolla, in 1985, 1986, and 1988, respectively.

He joined the Department of Electrical and Computer Engineering at the University of Florida, where he was an Assistant Professor from 1988 through 1993, and an Associate Professor from 1993 through 1998. In August 1998, he joined the

Electrical Engineering Department at Texas A&M University, College Station. He has also held visiting positions at Motorola Inc., the University of Utah, and UCSD. He has taught courses at both the graduate and undergraduate level on such topics as signals and systems, engineering mathematics, digital and analog communications, probability and random processes, coding, information theory, spread spectrum, detection and estimation theory, wireless communications, queueing theory and communication networks. He has published over 75 refereed journal and conference papers on a variety of topics in the area of digital communication theory. His current research interests include the area of wireless communications with a special emphasis on CDMA systems.

Dr. Miller is an Editor for the IEEE TRANSACTIONS ON COMMUNICATIONS.



**Mark J. Shensa** was born in Cleveland, OH, in 1944. He received the B.A. degree in mathematics from Princeton University, Princeton, NJ, in 1966, and the M.A. degree in mathematics and Ph.D. degree in electrical engineering from the University of California, Berkeley, in 1969 and 1971, respectively.

From 1971 to 1974, he was an Associate Professor of Applied Mathematics at IME in Rio de Janeiro, Brazil. In 1974, he joined Texas Instruments, Inc. Since 1980, he has been with NCCOSC in San Diego, CA. Previous work includes singular

perturbation theory, adaptive signal processing, tracking and localization, data fusion, Boolean logic, and wavelets. He worked for several years on wireless communications. His current interest includes network security and intrusion detection.

Dr. Shensa served as an Editor of the IEEE TRANSACTIONS ON ACOUSTICS, SPEECH, and SIGNAL PROCESSING from 1981 to 1984.



**Lawrence B. Milstein** (S'66–M'68–SM'77–F'85) received the B.E.E. degree from the City College of New York, New York, in 1964, and the M.S. and Ph.D. degrees in electrical engineering from the Polytechnic Institute of Brooklyn, Brooklyn, NY, in 1966 and 1968, respectively.

From 1968 to 1974, he was with the Space and Communications Group of Hughes Aircraft Company, and from 1974 to 1976, he was a Member of the Department of Electrical and Systems Engineering, Rensselaer Polytechnic Institute, Troy,

NY. Since 1976, he has been with the Department of Electrical and Computer Engineering, University of California at San Diego (UCSD), La Jolla, where he is a Professor and former Department Chairman, working in the area of digital communication theory with special emphasis on spread-spectrum communication systems. He has also been a consultant to both government and industry in the areas of radar and communications.

Dr. Milstein was an Associate Editor for Communications Theory for the IEEE TRANSACTIONS ON COMMUNICATIONS, an Associate Editor for Book Reviews for the IEEE TRANSACTIONS ON INFORMATION THEORY, an Associate Technical Editor for the IEEE COMMUNICATIONS MAGAZINE, and Editor-in-Chief of the IEEE JOURNAL ON SELECTED AREA IN COMMUNICATIONS. He was the Vice President for Technical Affairs in 1990 and 1991 of the IEEE Communications Society and the IEEE Information Theory Society. He has been a member of the IEEE Fellows Selection Committee since 1996, and he currently is the Chair of that committee. He is also the Chair of ComSoc's Strategic Planning Committee. He is a recipient of the 1998 Military Communications Conference Long-Term Technical Achievement Award, Academic Senate 1999 UCSD Distinguished Teaching Award, an IEEE Third Millennium Medal, 2000, and the 2000 IEEE Communication Society Armstrong Technical Achievement Award.